http://journal.uir.ac.id/index.php/JGEET

E-ISSN : 2541-5794
P-ISSN : 2503-216X

Journal of Geoscience,
Engineering, Environment, and Technology
Vol 8 No 1 2023

RESEARCH ARTICLE

Lineament Density and Implications for the Distribution of Ground Fissures After 2021 M_W 7.3 Flores Sea Earthquake on Kalaotoa Island, Indonesia

Baso Rezki Maulana [1,*], Muhammad Sulhuzair Burhanuddin [1,2], Muh. Fikri Akbar [3]

[1] *Geological Engineering, Hasanuddin University, Km.10 Makassar 90245, South Sulawesi, Indonesia.*
[2] *Graduate School of International Resources Sciences, Akita University, 28 - 2, Tegata - Gakuenmachi, Akita 010 - 8502, Japan.*
[3] *Undergraduate School of Geological Engineering, Hasanuddin University, Km.10 Makassar 90245, South Sulawesi, Indonesia.*

* Corresponding author: rezkimaulana@unhas.ac.id
Tel.: +62 82232268843
Received: Nov 1, 2022; Accepted: Mar 17, 2023.
DOI: 10.25299/jgeet.2023.8.1.10849

Abstract

A 7.3 M_W earthquake occurred at 11:20 am on December 14, 2021, in the Flores Sea, and the main shake was centered ±100 km north of Maumere, Indonesia, with a depth of 14.3 km, antecedent a landslide. This research consists of two stages, namely: quantitative data collection in the form of tectonic lineament density measurements using Shuttle Radar Topography Mission (SRTM) data which is extracted manually using GIS-based applications, and qualitative data in the form of field observations which include strike-dip measurements of rocks, lithological data, morphological conditions, ground fissures, and the distribution of damage caused after 2021 earthquake. This study focused on analyzing the value of lineament density, its correlation to the history of seismicity and surface lithological conditions, and the impact after the 2021 earthquake damage. The lineaments of the southern area are dominated by NE – SW orientation along with various lithological conditions and with lineament density values very low – very high. A crack width from 0.5 to 112 cm, and a vertical offset occurs with a depth of up to 270 cm. The western area is dominated by lineament with an orientation NE – SW with a crack width from 8 to 18 cm, and there is a vertical offset with a depth of up to 24 cm. The distribution of ground fissures in the Garaupa Raya area is categorized as low. The orientation of the northern area lineament is relatively NW – SE directional and the lineament density value is categorized as low. Horizontal displacement with an orientation of NW – SE is found at the port of Kalaotoa Island, Kawawo village with measured crack width of ±17 cm, an observable horizontal offset from 15 to 24 cm, and a vertical offset of ±12 cm with a trend of movement towards the south.

Keywords: 2021 Earthquake, Lineaments Density, Ground Fissures, Approximately Crack, Displacement

1. Introduction

The earthquake in the Flores Sea occurred at 11:20 am on December 14, 2021 (BMKG, 2021; USGS, 2021). Based on data on the location of the epicenter, depth, and focal mechanism from BMKG and USGS, the main shock focused on ±100 km north of Maumere City, Indonesia (122.200°E; 7.603°S), with an M_W 7.36 at a depth of 14.3 km (Fig. 10). The seismicity and tectonics of the Flores Sea thrust system (FSTS) consisting of the Flores Sea thrust, Selayar fault, and Kalaotoa fault have been reported by several researchers (e.g., Goes et al., 1997; Hall & Sevastjanova, 2012; Hutchings & Mooney, 2021; Supendi et al., 2020, 2022; Yang et al., 2020) This reverse fault once triggered an earthquake of M_W 7.8 at a depth of 27.7 km and triggered a tsunami wave as high as 25 m with a distribution radius of 300 m on 12/12/1992, at 01:29 pm.

Research on the condition of tectonic lineament density related to the history of seismicity, potential, and the impact of damage caused by the earthquake in the South Sulawesi area, especially on Kalaotoa Island, has not been done much. The position of the study site which is not far from the Kalaotoa fault, Selayar fault, and Flores Sea thrust, as well as the history of intensive and destructive seismicity (e.g., 2021 Flores Sea earthquake M_W 7.3) underlying this study to analyze the value of lineament density, correlation to the history of seismicity, and surface lithological conditions as well as the impact of after earthquake damage on December 14, 2021, that was exposed in the field.

2. Geological Setting

Kalaotoa Island is one of the outer islands of South Sulawesi composed of micro-continentals formed from tectonic activity during the Middle Miocene (Hall & Sevastjanova, 2012; Koswara et al., 1994).The study location is located in the Kalaotoa Island area, Pasilambena District, Selayar Islands Regency, South Sulawesi Province (121.74167° - 121.84167°E and 7.32917° - 7.42500°S) or ±40 km from the epicenter of 2021 Flores Sea earthquake. Sulawesi Island is divided into several tectonic provinces, namely: (1) West and North Sulawesi; Pluto-Volcanic arcs on the southern and northern arms of the island, (2) the Metamorphic Belt of Central Sulawesi; extending from the center of the island to the southeastern arm, (3) the Phospholite Belt of South Sulawesi on the eastern arm, and (4) fragments of the continents of Banggai-Sula and The Ironsmith (e.g., Kadarusman et al., 2004; Maulana et al., 2013, 2015). The stratigraphy of the study area is included in the Bonerate Sheet Geological Map, South Sulawesi. The oldest formation, the Kalao Formation (Tmk), consists of sandstones interfingering with marl and contact conglomerates which conformity with the Limestone

Member of Selayar Formation Limestone (Tms) consisting of sandstones and limestones. Members of the Selayar Formation Limestones are not aligned with Pleistocene – Holocene-aged rocks in the form of coral limestone (Ql) that are widespread in the northern part of the island (Koswara et al., 1994; Fig. 1).

The geological structures that developed in the study area were joints, strike-slip faults, and normal faults in the northwest-southeast and northeast-southwest directions. Fault structures and tectonic lineaments are recorded and can be interpreted through remote sensing imagery (e.g., satellite imagery, digital terrain model, and/or shuttle radar topography mission). The entire geological structure of Kalaotoa Island was formed at the beginning of the Middle Miocene and its peak at the time of the Pliocene – Pleistocene (Koswara et al., 1994; Supendi et al., 2022).

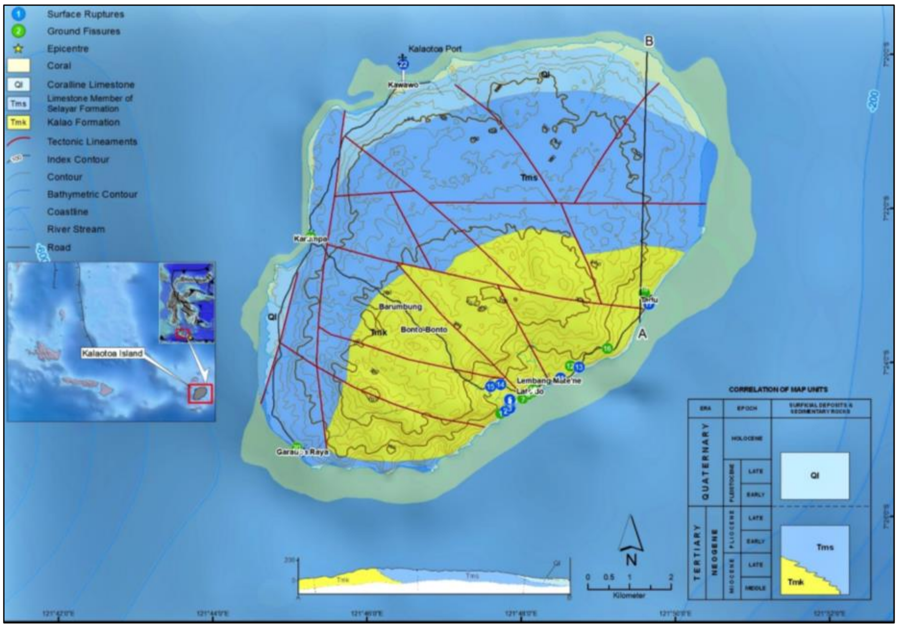

Fig. 1. Geological maps showing surface ruptures and ground fissures location distribution of Kalaotoa Island (modified after Koswara et al., 1994)

3. Methods

This research consists of two stages, namely: quantitative data collection in the form of tectonic lineament density measurements using Shuttle Radar Topography Mission (SRTM) data which is extracted manually using GIS-based applications, and qualitative data in the form of field observations which include strike-dip measurements of rocks, lithological data, morphological conditions, ground fissures, and the distribution of damage caused after 2021 earthquake. All data from GIS interpretation and field observations are then compiled for further analysis and interpretation. Data collection in the study area after the 2021 earthquake was carried out by measuring the direction of the trend, and the dimensions of the fracturing (length and the crack width). In addition, we took several rock samples that could representatively represent lithological formations in the study area. Field measurement data is carried out using field survey tools according to geological standards such as GPS hand-held, compass, clinometer, and tape measure.

Lineament on the earth's surface can be a manifestation of the conditions of subsurface geological structures that also reflect tectonic processes in the earth's crust and as an indication of geological disasters (Iqbal & Juliarka, 2019). Through satellite imagery data, the lineament can be shown as a line that is lighter or darker than the background. (Han et al., 2018). In the process of lineament density analysis, some factors that affect the results of the analysis are secondary data and imagery data such as DEM with a certain resolution. High-resolution data imagery such as IFSAR DEM with a resolution of 5 m, SRTM with a resolution of 30 and 90 m, and ASTER GDEM with a resolution of 30 m are very appropriate to be used in declining tectonic lineament (Verdiansyah et al., 2017). The lineament density is a measure of the density and frequency of each lineament unit of each regional area (Zhumabek et al., 2017).

Lineament data were analyzed using frequency, length, rose diagram, and/or density map data. Lineament density is determined by utilizing the total lineament length per unit area (Bety et al., 2022). Lineament density mapping is performed by delineating tectonic lineament using DEM-SRTM. The data used is a Digital Elevation Model (DEM) based on Shuttle Radar Topography Mission (SRTM) 1 arc/sec (https://earthexplorer.usgs.gov/) and Batimetri Nasional (BATNAS) 3 arc/sec global resolution (https://tanahair.indonesia.go.id/demnas/#/batnas). The DEM is used to visualize the tectonic distribution of the Kalaotoa Island lineament to provide a vertical reflection of the image to bring out faults and/or folds below the surface. Lineament delineation on DEM is extracted manually using Quantum GIS (https://www.qgis.org/en/site/index.html) software. Considering the quality of high-resolution DEM is much better than satellite imagery (Batson et al., 1975).

This method is carried out to calculate the level of density and the magnitude of the lineament frequency in an area. The identified data components include dimensions, bearings, and lineament density. The classification of the lineament density map is based on the Thannoun Lineament Density classification (2013), on this basis, the study location is divided into several classes based on the frequency of the lineament. Field survey data and spatial analysis, including ground fissures and surface rupture zones trends, bearing of lineament, dip direction of rupture plane, and strike-dip, were processed using GeoRose software (https://www.yongtechnology.com/georose/) to determine fault, lineaments, and vertical displacements orientations on Kalaotoa Island (Fig. 9; Table 1 and 2). The lineament density map that has been made is then combined with regional geological structure data and field survey data to determine the relationship between the lineament density value to the distribution, the direction of ground fissures orientation after the 2021 earthquake, lithological conditions, and fault orientation that develops in the Kalaotoa Island.

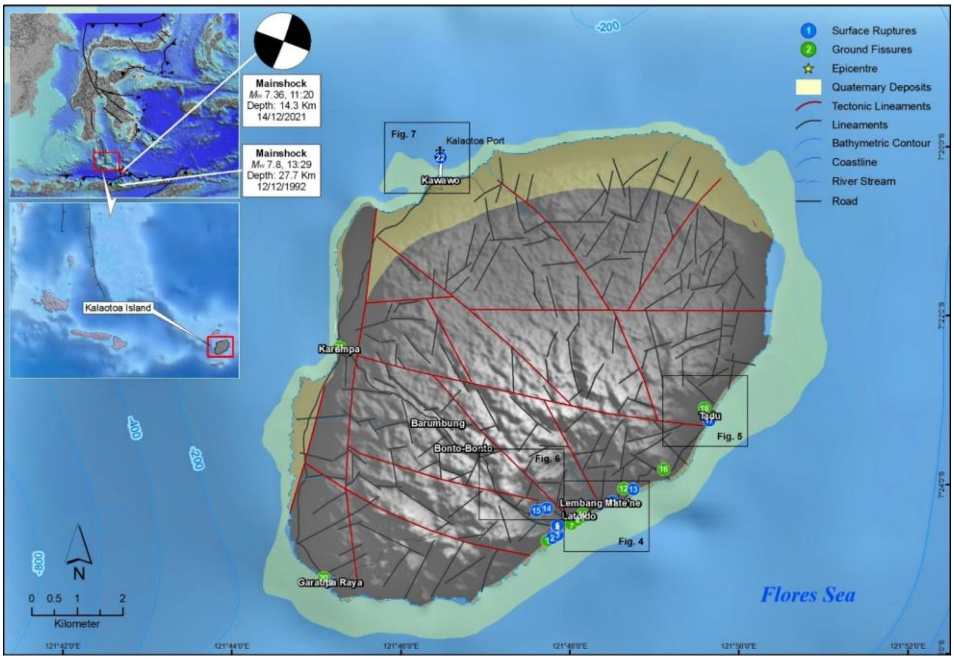

Fig. 2. Elevation maps showing tectonic lineaments and observation location in Kalaotoa Island after the 2021 Flores Sea earthquake. The base map is a compilation of 1 arc/sec DEM-SRTM (USGS) and 3 arc/sec DEM (BATNAS, BIG).

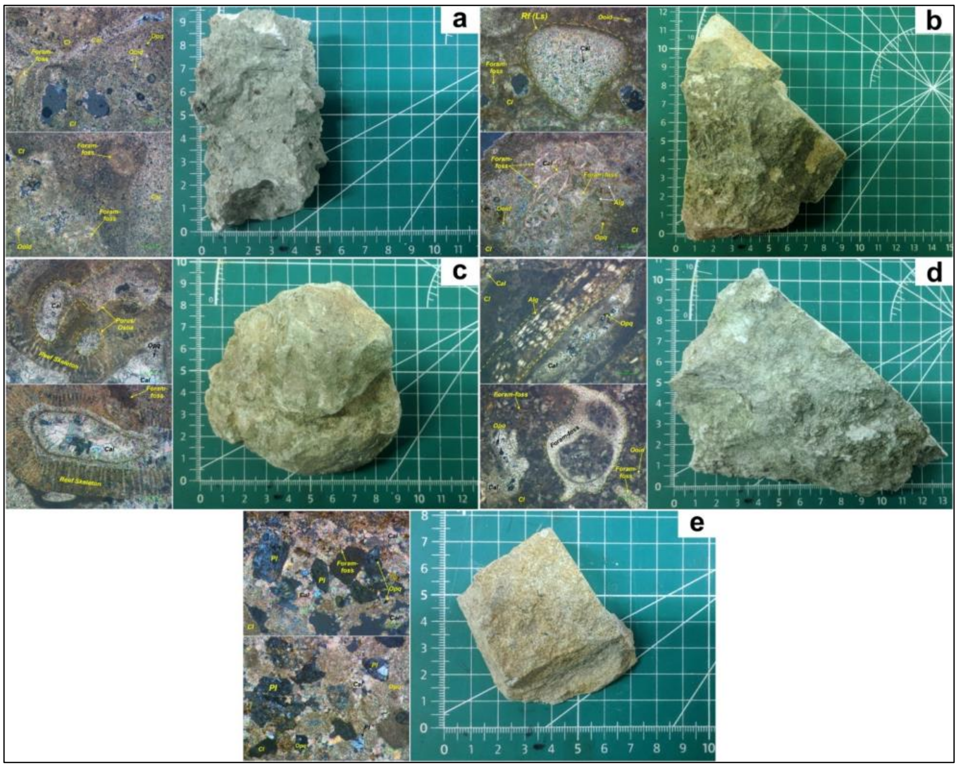

Fig. 3. Photomicrographs with zoom level 50x and rock samples in Kalaotoa Island. a-b) Packstone samples, location in KL_01 and KL_04, Lato'do village; c) Boundstone samples, location in KL_14, Bonto-Bonto village; d) Packstone samples, location in KL_19, Garaupa Raya village; e) Grainstone samples, location in KL_25, Lembang Mate'ne village.

4. Results

4.1 The Southern (Lato'do – Lembang Mate'ne – Bonto-Bonto – Tadu) Area

Based on the results of spatial data processing, the southern area lineament is dominated by NE – SW orientation. The resulting lineament density map shows that the southern area is divided into several classes based on their lineament density. Approximately 7 km^2 of the southern area is an area with a density value of very low; 11.5 km^2 low; 9.8 km^2 moderate; 4.7 km^2 high; and 1.2 km^2 very high with a total area of approximately 34.2 km^2. Based on these data clusters, the lineament density value in the southern area varies greatly from very low – very high (Fig. 9; Table 1 and 2).

In general, there are 18 observation points of ground fissures, locally there are surface ruptures, and subsidence scattered in the villages of Lato'do, Lembang Mate'ne, Bonto-Bonto, and Tadu so that they cross several residential areas, roads, and coastlines in the southern and southeastern parts of Kalaotoa Island. Ground fissures in the Lato'do village have a dominant orientation direction of NW – SE which is not in the direction of the fault orientation, the width of the crack is 0.5 to 57 cm, and there is a vertical offset with a depth of up to 250 cm. Ground fissures observed in the Lembang Mate'ne village are oriented NE – SE with a crack width of 1.7 to 87 cm and a vertical offset with a maximum depth of 4 to 270 cm. Ground fissures observed in Bonto-Bonto village were 2 points with the direction of the dominant orientation of NW – SE almost parallel with the western fault in Kalaotoa with a total length of approximately 4 m, an approximately crack width of 8 to 112 cm, and a vertical offset with a maximum height of 32 cm. In Tadu village the orientation of ground fissures is relatively NE – SSW directional, has a crack width of 2 to 41 cm, and vertical offset reaches 16 cm. The character of this fracturing is branching, in some places cut off or covered by avalanche material, and several continuously towards the S – SE part of the island. Ground fissures in this area generally intersect or continuously in the direction of the village road, especially along the southeastern coastline, thus damaging the access to the land route of the eastern and southern parts of Kalaotoa Island (Fig. 2, 4-6; Table 1).

Table 1. Fractures data of the 14 December 2021 Flores Sea earthquake in Kalaotoa Island.

No	Location	Longitude	Latitude	Trend of Ground Fissure* & Rupture Zone (Clockwise from N)	Fracture Zone Width (cm)	Horizontal Displacement (cm) & Slip Sense		Vertical Displacement (cm) & Downward Block	
				SOUTHERN AREA					
1	KL_01	121.796°E	7.411°S	310	2	–	–	0.2 – 0.8	S
2	KL_02	121.797°E	7.411°S	62; 100; 290	0.5 – 1.4	–	–	0.4 – 1.2	S
3	KL_03	121.798°E	7.410°S	120; 157	1 – 8	–	–	05 – 11	S
4	KL_05	121.798°E	7.409°S	33; 80; 110	32	–	–	60	S
5	KL_06	121.798°E	7.408°S	205; 210; 242; 264; 283	1 – 5	–	–	100 – 250	W
6	KL_07	121.798°E	7.408°S	40; 130; 57; 84	8	–	–	72	S
7	KL_08	121.800°E	7.408°S	140	30	–	–	28	S
8	KL_09	121.801°E	7.407°S	174	0.7 – 2.1	–	–	60 – 80	S
9	KL_10	121.803°E	7.406°S	127; 132; 144; 151	30	–	–	1.8 – 2.7	E
10	KL_11	121.803°E	7.406°S	34; 66; 94; 103	57	–	–	0.5 – 2	S
11	KL_24	121.808°E	7.403°S	100	15	–	–	20 – 34	S
12	KL_25	121.811°E	7.401°S	104; 166	1.7 – 2.9	–	–	182 – 270	S
13	KL_26	121.813°E	7.401°S	132; 143; 156	32 – 87	–	–	04 – 12	S
14	KL_12	121.795°E	7.405°S	75; 79; 84	14 – 112	–	–	16 – 32	S
15	KL_13	121.793°E	7.405°S	46; 50; 63; 103; 109; 117; 130; 134	27	–	–	127 – 184	S
16	KL_27	121.819°E	7.397°S	284	2 – 18	–	–	0.7 – 1	E
17	KL_28	121.828°E	7.387°S	281	7	–	–	1.4 – 2.1	W
18	KL_29	121.827°E	7.385°S	265	17 – 41	–	–	3 – 18	S
				WESTERN AREA					
19	KL_21	121.753°E	7.419°S	108; 314; 327	8 – 14	–	–	7 – 15	S
20	KL_23	121.751°E	7.418°S	320; 332	10 – 1 8	–	–	24	E
				NORTHERN AREA					
21	KL_20	121.755°E	7.373°S	268	10	–	–	5	W
22	KL_30	121.775°E	7.336°S	18; 20; 59	10 – 17	15 – 24	Dextral	0 – 12	S

*Bold number: Ground fissure confirmed

Fig. 4. a) A surface rupture cutting a road at Lato'do village. b-c) Ground fissures at Lato'do village.

Fig. 5. a) Lithology component at Lembang Mate'ne-Tadu area. b-c) Ground fissures cutting a road at Tadu village.

The constituent lithology of this area is carbonate sedimentary rocks (grainstone, packstone, and boundstone). In the thin section, grainstone is mainly composed of skeletal grains (foraminifera fossil 23-31%), non-skeletal grains (plagioclase 30-38% and ooid 9-12%), opaque minerals (1-3%), clay minerals (<3-5%), and calcite (21-27%), material components measuring <0.02-2.48 mm with a subangular – rounded shape, medium-coarse clastic texture, closed packaging, medium sorting, and layered rock structure (locally showing the structure of the rock parallel and convoluted lamination). The presence of lamination structures and plagioclase minerals as components of grainstone material is an early indication that carbonate sedimentary rocks in this area are composed of fragments of older igneous rocks (e.g., Kayuadi Formation/Tmok) and with a transitional deposition environment to shallow seas. Based on the geographical location and physical characteristics of lithology, this rock is thought to be part of the Central Miocene-aged Kalao Formation. Packstone is mainly composed of skeletal grains (foraminifera and algae fossil 37-42%), non-skeletal grains (ooid 10-12%), opaque minerals (<2%), clay minerals (8-14%), and calcite (29-32%), material components measuring <0.02-4.18 mm with angular – subrounded shapes, medium-coarse clastic textures, open packaging, poor sorting, and non-layered rock structures. Based on the physical characteristics of lithology and the presence of fossils of *Orbulina universa* D'ORBIGNY and *Sphaerodinelopsis sp.* indicates that this rock is part of the Limestone Member of Selayar Formation which is of Middle Miocene – Pliocene age and with a depositional environment in the form of shallow seas. In addition, in some locations (hilly areas of Bonto-Bonto village) there are outcrops of carbonate sedimentary rocks (boundstones) with physical characteristics composed of corals and have undergone a process of diagenesis characterized by calcite minerals that fill fracturing and pores in rocks (Fig. 1, 3a- c, e, and 5a).

Based on data from field observations after the 2021 earthquake and laboratory analysis, it is interpreted that the constituent rocks in this area are members of the Kalao Formation (Tmk) and Limestone Members of the Selayar Formation (Tms) with moderate to high weathering levels, layered rock structures, intercalations of marl and conglomerate, and in some places are massive. Southern areas have very low – very high lineament density values, but the distribution of ground fissures is dominant in the Lato'do, Lembang Mate'ne, and Bonto-Bonto areas which are composed of packstone and boundstone members of the Kalao Formation with the high level of weathering while in some areas closer to the epicenter, especially Tadu villages with grainstone lithology, low erosion rates, and a relatively flat elevation – undulating terms subject to significant impacts (Fig. 2, 9, and 10).

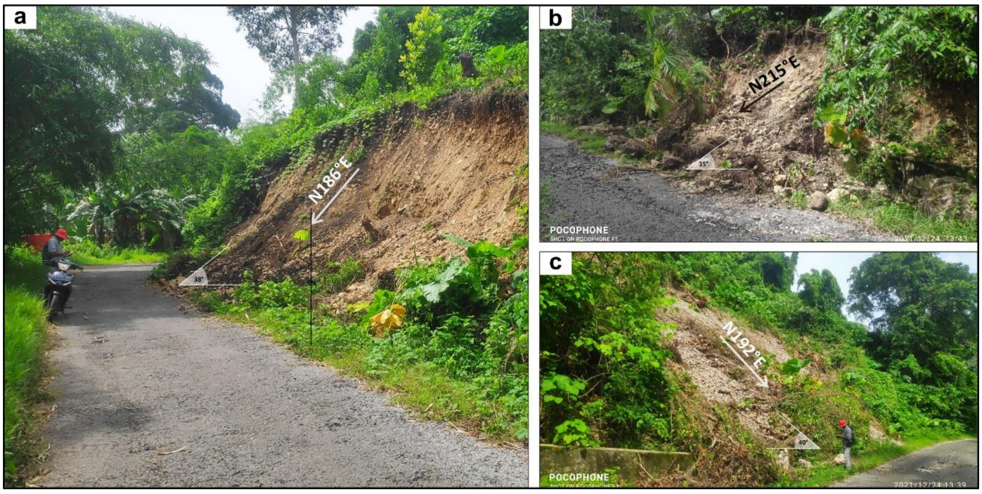

Fig. 6. a-c) Landslide site in Bonto-Bonto village with avalanche material component in the form of limestone fragments (calcarenite/packstone).

4.2 The Western (Garaupa Raya) Area

The Western area is dominated by lineaments and ground fissures with NE – SW orientation. The resulting lineament density map shows that the western area is divided into several classes based on its lineament density. Approximately 3.5 km^2 of the western area is an area with a density value of very low; 9.3 km^2 low; 7 km^2 moderate; 1.5 km^2 high; and <1 km^2 very high with a total area of approximately 21 km^2. Based on these data clusters, the western area has a low – moderate lineament density value (Fig. 9; Table 1 and 2).

In general, there are 2 observation points of ground fissures, locally there are surface ruptures, and subsidence scattered in the Garaupa Raya village so that it crosses several residential areas, roads, and coastlines of the western part of Kalaotoa Island. Ground fissures in this area have a dominant orientation in the direction NE – SW, a crack width of 8 to 18 cm, and there is a vertical offset with a depth of up to 24 cm. The character of this fracturing is branching, in some places cut off or covered with sedimentary material, and some continuously towards the S – SW part of the island. Ground fissures in this area generally intersect or continue in the direction of the village road, especially along the coastline of the western part of Kalaotoa Island (Fig. 2; Table 1).

The constituent lithology of this area is carbonate sedimentary rocks (packstone). In the thin section, packstone is mainly composed of skeletal grains (foraminifera and algae fossil 22-34%), non-skeletal grains (ooid 10-15%), opaque minerals (<3%), clay minerals (18-21%), and calcite (17-29%), material components measuring <0.02-3.27 mm with angular – subrounded forms, medium-coarse clastic texture, open packaging, poor sorting, and layered rock structure. Based on the physical characteristics of lithology and the presence of fossils *of Orbulina universa* D'ORBIGNY and *Sphaerodinelopsis sp.* indicates that this rock is part of the Limestone Member of Selayar Formation which is middle Miocene – Pliocene age and with a depositional environment in the form of shallow seas (Fig. 1, 3d, and 7).

Based on data from field observations and laboratory analysis, it is interpreted that the constituent rocks in this area are Limestone Members of the Selayar Formation (Tms) with moderate to high weathering levels, layered rock structures, intercalations of marl, and conglomerates. The distribution of ground fissures in the Garaupa Raya area is composed of packstones with high weathering levels and the thick coastal sedimentary cover is categorized as low (Fig. 2, 9, and 10; Table 1 and 2).

Fig. 7. Carbonate sedimentary rocks outcrop at Garaupa Raya village.

4.3 The Northern (Karumpa – Kawawo) Area

The orientation of the northern area lineament is relatively NW – SE directional. The resulting lineament density processing results show that the northern area is divided into several classes based on lineament density. Approximately 7.3 km^2 of the northern area is an area with a density value of very low; 11.5 km^2 low; 4.8 km^2 moderate; 1 km^2 high; and <1 km^2 very high or with a total area of approximately 24 km^2.

The results of field observations after the 2021 earthquake and laboratory analysis, this area was composed of Pleistocene-aged coralline limestone (Ql) and coastal alluvial deposits with moderate to high weathering levels, and non-layered rock structures. Based on these data clusters, the northern area broadly has a very low – low lineament density value where the distribution of ground fissures in this area is categorized as low. A horizontal shift with an NW – SE orientation is found on the port of Kalaotoa island, Kawawo village. This shift is accompanied by a crack of ±17 cm (a shift observed in the structure of the Kalaotoa Island port building), an observable horizontal action of 15-24 cm, and a vertical offset of ±12 cm with an orientation of movement toward the south. The fracturing on the Kalaotoa Island port is interpreted to extend eastward to southeastwards which has a higher lineament density value (Fig. 2, 8-10; Table 1 and 2).

Table 2. Fractures data of the 14 December 2021 Flores Sea earthquake in Kalaotoa Island.

Density Level	Area	Wide (Km^2)	Perimeter (Km)
Very Low	Southern Area	7.38	46.02
	Northern Area	9.37	31.69
	Western Area	3.35	29.67
Low	Southern Area	11.45	80.97
	Northern Area	7.17	45.10
	Western Area	9.42	56.00
Moderate	Southern Area	9.78	79.53
	Northern Area	4.92	32.96
	Western Area	6.69	45.97
Strong	Southern Area	5.20	38.14
	Northern Area	1.04	9.87
	Western Area	1.29	9.42
Very Strong	Southern Area	1.05	10.10
	Northern Area	0.02	0.71
	Western Area	0.01	0.45

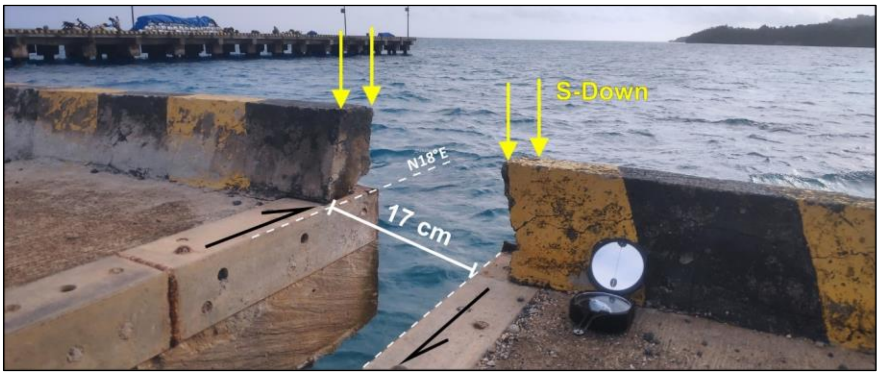

Fig. 8. A surface rupture cutting a road to Kalaotoa Port, Kawawo village.

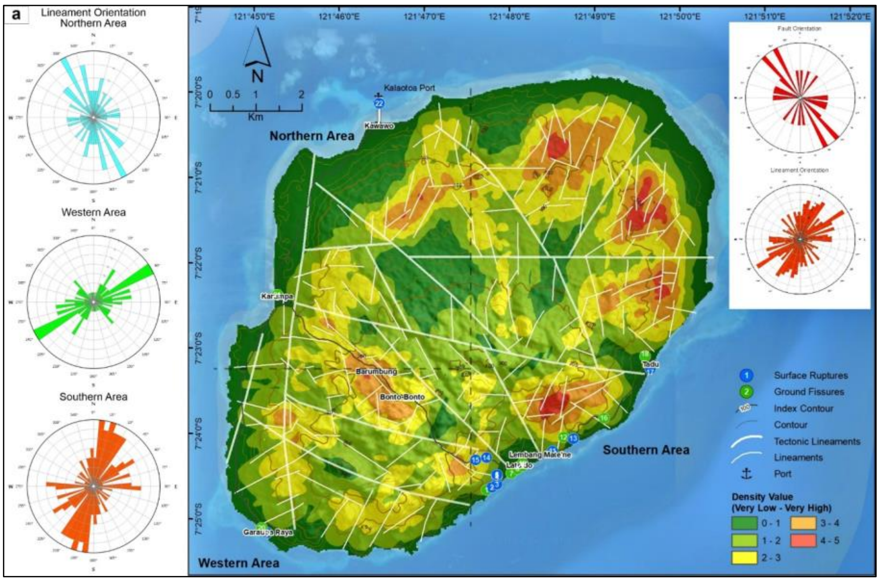

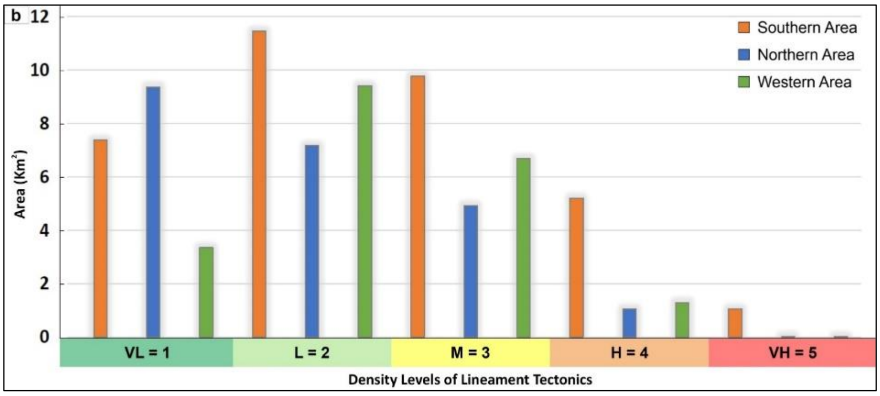

Fig. 9. a) Density maps showing orientation and density value of lineament compared with fault orientation in Kalaotoa Island, we divide into three zones based on the density value and distribution of the ground fissures after the 2021 earthquake. b) Density levels of lineament tectonics in Kalaotoa Island. The orange column is the southern area, the blue column is the northern area, and the green column is the western area of the study area.

5. Discussion

Various methods can also determine the cause of an earthquake, one of them is the HVSR method using amplification value. The greater the difference in values, the greater the magnification experienced by the wave (Arifin et al., 2014). The comparison of the impedance contrast of the surface layer to the layer below is related to the value of the surface amplification factor, where if the contrast ratio of the impedance of the two layers is high the value of the strengthening factor is also high, resulting in a difference in the frequency of lineament in an area (Nakamura, 2000). Amplification occurs when an object that has its frequency is disturbed by the propagation of other waves with the same or different frequencies so that the effect caused can vary with an uneven distribution (e.g., the impact of earthquake damage on an area can vary depending on lithological conditions and patterns of geological structure). From the results of observations and laboratory analysis, we assume and interpret that the implications of lineament density values and distances from epicenters are also controlled by geological conditions such as physical and chemical properties of lithology, soil thickness/ surface sediment deposits, and topography. Evidenced by the condition of the study site after the 2021 earthquake M_W 7.3 located in the Flores Sea (±40 km from the study site) where the southern area is composed of carbonate sedimentary rocks that are not massive with very high lineament density values are strongly affected. However, on the east side (north of Tadu village) which has a lineament density value of high – very high, it diverges and has a very low damage impact compared to the Kawawo area which has a lower density value (Fig. 10).

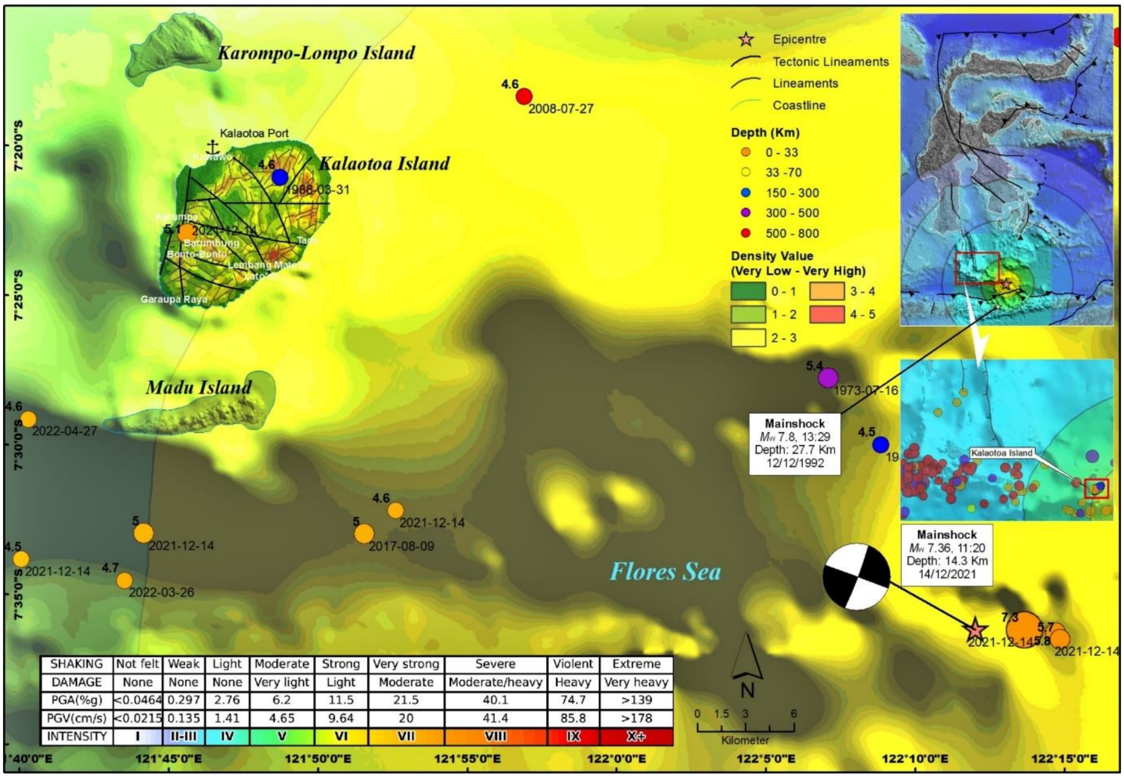

Fig. 10. Density maps overlay Seismicity of the South Sulawesi and Flores Sea area. Epicenters of moderate and large events (M_W 4–8) that occurred in shallow depth (<800 km) from 1962 to 2021 are shown. Magnitude source: Hutchings & Mooney, 2021; Supendi et al., 2020, 2022; Yang et al., 2020; and Indonesian Earthquake Catalog, the based map: peak ground acceleration (PGA) by USGS (2021). Structural lineaments are drawn after (Koswara et al., 1994 ; Supendi et al., 2022)

6. Conclusion

The lineaments of the southern area are dominated by NE – SW orientation along with various lithological conditions and with lineament density values very low – very high. A crack width from 0.5 to 112 cm, and a vertical offset occurs with a depth of up to 270 cm. The western area is dominated by lineament with an orientation NE – SW with a crack width from 8 to 18 cm, and there is a vertical offset with a depth of up to 24 cm. The character of this fracturing is branching, in some places cut off or covered by avalanche material, and several continuously towards the S – SE part of the island.

The Western area is dominated by lineaments and ground fissures with NE – SW orientation. The width of the fissures cracks is from 8 to 18 cm, and there is a vertical offset with a depth of up to 24 cm. The character of this fracturing is branching, in some places cut off or covered with sedimentary material, and some continuously towards the S – SW part of the island. The distribution of ground fissures in the Garaupa Raya area is categorized as low.

The orientation of the northern area lineament is relatively NW – SE directional and the lineament density value is categorized as low. Horizontal displacement with an orientation of NW – SE is found at the port of Kalaotoa Island, Kawawo village with measured crack width of ±17 cm, an observable horizontal offset from 15 to 24 cm, and a vertical offset of ±12 cm with a trend of movement towards the south.

The highest damage caused by the earthquake is located in a southern area which is shown by the high volume of ground fissures and the occurrence of land subsidence alongside the coastline of the southern area of Kalaotoa Island. This damage is also clarified by a very high value of density lineament in the southern area specifically in Lembang Mate'ne.

Acknowledgments

We are concerned for the people of Selayar Island and the victims of this earthquake. We thank the Ministry of Higher Education of Indonesia, the Center of Volcanology and Geological Hazard Mitigation, the Indonesian Association of Geologists, and Hasanuddin University for providing a research grant. We also thank the Geological Engineering Department students at Hasanuddin University (Gowa) for supporting us during the field survey.

References

Arifin, S. S., Mulyatno, B. S., Marjiyono, & Setianegara, R. (2014). Penentuan Zona Rawan Guncangan Bencana Gempa Bumi Berdasarkan Analisis Nilai Amplifikasi HVSR Mikrotremor dan Analisis Periode Dominan Daerah Liwa dan Sekitarnya. Jurnal Geofisika Eksplorasi, 2(1). https://doi.org/10.23960/jge.v2i01.217

Batson, R. M., Edwards, K., & Eliason, E. M. (1975). Computer-generated shaded-relief images. Journal of Research US Geology Survey, 3(4), 401–408.

Bety, A. K. S., Al-Jawadi, A. S., & Ismaeel, O. A. (2022). Lineament Analysis by Using Remote Sensing and GIS Technique of Sangaw Area, Kurdistan Region, NE Iraq. Iraqi Geological Journal, 55(2), 150–161. https://doi.org/10.46717/igj.55.2C.11ms-2022-08-24

BMKG (2021). Ulasan Guncangan Tanah Akibat Gempa Bumi di Laut Flores Nusa Tenggara Timur 14 Desember 2021. URL https://www.bmkg.go.id/berita/?p=ulasan-guncangan-tanah-akibat-gempa-bumi-di-laut-flores-nusa-tenggara-timur-14-desember-2021&lang=ID&tag=gempabumi (accessed 20.12.21).

Goes, S., Ruff, L., & Winslow, N. (1997). The Complex Rupture Process of the 1996 Deep Flores, Indonesia Earthquake (Mw 7.9) from teleseismic P-waves. Geophysical Research Letters, 24(11), 1295–1298.

Hall, R., & Sevastjanova, I. (2012). Australian crust in Indonesia. Australian Journal of Earth Sciences, 59(6), 827–844. https://doi.org/10.1080/08120099.2012.692335

Han, L., Liu, Z., Ning, Y., & Zhao, Z. (2018). Extraction and analysis of geological lineaments combining a DEM and remote sensing images from the northern Baoji loess area. Advances in Space Research, 62(9), 2480–2493. https://doi.org/10.1016/j.asr.2018.07.030

Hutchings, S. J., & Mooney, W. D. (2021). The Seismicity of Indonesia and Tectonic Implications. https://doi.org/10.1029/2021GC009812

Iqbal, M., & Juliarka, B. R. (2019). Analisis Kerapatan Kelurusan (Lineament Density) di Lapangan Panasbumi Suoh-Sekincau, Lampung. Journal of Science and Applicative Technology, 3(2), 61. https://doi.org/10.35472/jsat.v3i2.212

Kadarusman, A., Miyashita, S., Maruyama, S., Parkinson, C. D., & Ishikawa, A. (2004). Petrology, geochemistry and paleogeographic reconstruction of the East Sulawesi Ophiolite, Indonesia. Tectonophysics, 392(1–4), 55–83. https://doi.org/10.1016/j.tecto.2004.04.008

Koswara, A., Panggabean, H., Baharuddin, & Sukarna, D. (1994). Geological map of the Bonerate Sheet, South Sulawesi, Scale 1:250 000 (Quadrangles 2018-2019-2208). Geological Research and Development Centre.

Maulana, A., Christy, A. G., & Ellis, D. J. (2015). Petrology, geochemistry and tectonic significance of serpentinized ultramafic rocks from the South Arm of Sulawesi, Indonesia. Chemie Der Erde, 75(1), 73–87. https://doi.org/10.1016/j.chemer.2014.09.003

Maulana, A., Christy, A. G., Ellis, D. J., Imai, A., & Watanabe, K. (2013). Geochemistry of eclogite- and blueschist-facies rocks from the bantimala complex, south sulawesi, indonesia: Protolith origin and tectonic setting. Island Arc, 22(4), 427–452. https://doi.org/10.1111/iar.12037

Nakamura, Y. (2000). Clear identification of fundamental idea of Nakamura's technique and its applications. Proceedings of the 12th World Conference on Earthquake Engineering, Auckland, New Zealand 2656, 1-8.

Supendi, P., Nugraha, A. D., Widiyantoro, S., Abdullah, C. I., Rawlinson, N., Cummins, P. R., Harris, C. W., Roosmawati, N., & Miller, M. S. (2020). Fate of Forearc Lithosphere at Arc-Continent Collision Zones: Evidence From Local Earthquake Tomography of the Sunda-Banda Arc Transition, Indonesia. Geophysical Research Letters, 47(6), 1-9. https://doi.org/10.1029/2019GL086472

Supendi, P., Rawlinson, N., Prayitno, B. S., Widiyantoro, S., Simanjuntak, A., Palgunadi, K. H., Kurniawan, A., Marliyani, G. I., Nugraha, A. D., Daryono, D., Anugrah, S. D., Fatchurochman, I., Gunawan, M. T., Sadly, M., Adi, S. P., Karnawati, D., & Arimuko, A. (2022). The Kalaotoa Fault: A Newly Identified Fault that Generated the Mw 7.3 Flores Sea Earthquake. The

Seismic Record, 2(3), 176–185. https://doi.org/10.1785/0320220015

USGS (2021). Earthhquakes. URL https://earthquake.usgs.gov/earthquakes/eventpage/us6000gc2a/executive (accessed 20.12. 21).

Verdiansyah, O., & Hartono, H. G. (2017). Aplikasi Lineament Density Analysis Untuk Membatasi Pola Kaldera Purba Godean. Jurnal Teknologi Technoscientia 9(2), 162–171. https://doi.org/10.34151/technoscientia.v9i2.137

Yang, X., Singh, S. C., & Tripathi, A. (2020). Did the Flores backarc thrust rupture offshore during the 2018 Lombok earthquake sequence in Indonesia. Geophysical Journal International, 221, 758–768. https://doi.org/10.1093/gji/ggaa018

Zhumabek, Z., Assylkhan, B., Alexandr, F., Dinara, T., & Altynay, K. (2017). Automated lineament analysis to assess the geodynamic activity areas. Procedia Computer Science, 121, 699–706. https://doi.org/10.1016/j.procs.2017.11.091